VIP Lithium-Ion Batteries Very Important Paper

DOI: 10.1002/ange.201402388

Elastic and Wearable Wire-Shaped Lithium-Ion Battery with High Electrochemical Performance**

Jing Ren, Ye Zhang, Wenyu Bai, Xuli Chen, Zhitao Zhang, Xin Fang, Wei Weng, Yonggang Wang, and Huisheng Peng**

Abstract: *A stretchable wire-shaped lithium-ion battery is produced from two aligned multi-walled carbon nanotube/lithium oxide composite yarns as the anode and cathode without extra current collectors and binders. The two composite yarns can be well paired to obtain a safe battery with superior electrochemical properties, such as energy densities of 27 Wh kg^{-1} or 17.7 mWh cm^{-3} and power densities of 880 W kg^{-1} or 0.56 W cm^{-3}, which are an order of magnitude higher than the densities reported for lithium thin-film batteries. These wire-shaped batteries are flexible and light, and 97% of their capacity was maintained after 1000 bending cycles. They are also very elastic as they are based on a modified spring structure, and 84% of the capacity was maintained after stretching for 200 cycles at a strain of 100%. Furthermore, these novel wire-shaped batteries have been woven into lightweight, flexible, and stretchable battery textiles, which reveals possible large-scale applications.*

Flexible, portable, wearable, and stretchable electronic devices have gained enormous popularity in recent years.[1–8] Motivated by the ever-growing market requirements, many conceptually new products, such as flexible smart phones, intelligent bracelets, and Google Glasses, appear as state-of-the-art technology and create a new world where people can acquire information in a few blinks. To this end, a suitable power system is desperately required and desired to power the above-mentioned electronic devices, which remains a challenge. Wire-shaped electrochemical storage devices that are flexible and can be woven into textiles have emerged and thrived in response.[9–14] Some efforts have been made to explore wire-shaped electrochemical supercapacitors by twisting two fiber electrodes; however, inferior performances, including low energy densities, prevented them from appearing on the market.[9–12] Instead, lithium-ion batteries with much higher energy densities are believed to become a probable replacement.[15] Wire-shaped lithium-ion batteries are not available because their use is prevented by several serious and critical obstacles, such as safety. The safety issues associated with lithium batteries have been previously discussed[9,15–18] and loom large for flexible wire-shaped batteries, especially when they are stretched and distorted during use.

The safety issue primarily arises from the growth of dendritic lithium on the anode surface especially during the over-charge process, as the lithiation potential approaches 0 V (vs. Li/Li$^+$) for conventional graphite, silicon, and alloy anodes.[19,20] The dendritic lithium on the anode will lead to a short circuit, and a lot of heat may be produced, leading to combustion. To avoid this problem, much attention has been paid to the development of new materials with higher lithiation potentials that can be employed as the anodes. Spinel $Li_4Ti_5O_{12}$ (LTO) has previously been investigated as a promising candidate as the insertion of Li ions can take place at approximately 1.5 V (vs. Li/Li$^+$).[21,22] Furthermore, spinel LTO and $LiMn_2O_4$ (LMO) also exhibit very small volume changes during cycling with a remarkable stability.[21,23–25] With a slight safety hazard, LTO-based planar batteries, such as LTO/LMO and LTO/$LiCoO_2$, are being commercialized for electric vehicles and energy storage stations.

Herein, novel and safe wire-shaped lithium-ion batteries that are lightweight and highly flexible and feature a high energy density were fabricated and investigated. They were made by embracing LTO and LMO nanoparticles into two aligned multi-walled carbon nanotube (MWCNT) yarns that serve as anode and cathode, respectively (Figure 1). Because of the aligned nanostructure and high electrical conductivity, no current collector and binders are required during the fabrication. The MWCNT/LTO and MWCNT/LMO composite yarns can be paired as anode and cathode to create a battery with remarkable electrochemical performance, which does not suffer from any safety issues. The wire-shaped battery, with a linear density of 12 mg m^{-1}, typically exhibits an energy density of 27 Wh kg^{-1} or 17.7 mWh cm^{-3} and a power density of 880 W kg^{-1} or 0.56 W cm^{-3}. The power density is one order of magnitude larger than that of the lithium thin-film batteries (10^{-2}–10^{-3} W cm^{-3}).[26] The calcu-

[*] J. Ren,[+] Y. Zhang,[+] W. Bai, X. Chen, Z. Zhang, X. Fang, W. Weng, Prof. H. Peng
State Key Laboratory of Molecular Engineering of Polymers, Department of Macromolecular Science, and Laboratory of Advanced Materials, Fudan University
Shanghai 200438 (China)
E-mail: penghs@fudan.edu.cn
Dr. Y. Wang
Department of Chemistry and Shanghai Key Laboratory of Molecular Catalysis and Innovative Materials
Institute of New Energy, Fudan University
Shanghai 200438 (China)
E-mail: ygwang@fudan.edu.cn
[+] These authors contributed equally to this work.

[**] This work was supported by MOST (2011CB932503), NSFC (21225417), STCSM (12nm0503200), the Fok Ying Tong Education Foundation, the Program for Special Appointments of Professors at Shanghai Institutions of Higher Learning, and the Program for Outstanding Young Scholars from the Organization Department of the CPC Central Committee.
Supporting information for this article is available on the WWW under http://dx.doi.org/10.1002/anie.201402388.

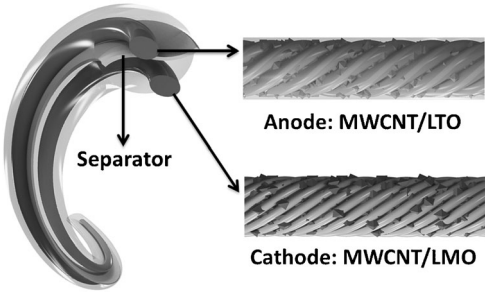

Figure 1. Structure of the flexible wire-shaped lithium-ion battery. The aligned MWCNT/LTO and MWCNT/LMO composite yarns are paired as the anode and cathode, respectively.

lations of all of these numbers were based on the overall volume of the electrode materials of the full battery. The wire-shaped battery was flexible and able to sustain thousands of repeated deformations with only a small decrease in capacity: The capacity remained at 97% after bending for 1000 cycles. The wire-shaped battery was further made into a spring structure to obtain a very elastic device. The capacity remained at 84% after the elastic battery had been stretched by 100% for 200 cycles.

Aligned MWCNT sheets were first drawn out from spinnable MWCNT arrays that had been synthesized by chemical vapor deposition.[13] LTO nanoparticles were synthesized through a solid-state method followed by ball milling,[27] and the LMO nanoparticles were synthesized by a hydrothermal method.[28] Both LTO and LMO nanoparticles exhibited diameters of hundreds of nanometers (Supporting Information, Figure S1), and a spinel structure that was validated by the X-ray diffraction pattern (Figure S2). Aligned MWCNT/LTO and MWCNT/LMO composite yarn electrodes were prepared by coating LTO and LMO nanoparticles onto the MWCNT sheet, followed by twisting of the resulting composite films. Scanning electron microscopy (SEM) images of the two composite yarns are shown in Figure 2. The MWCNT/LTO and MWCNT/LMO composite yarns exhibited uniform diameters of 70 and 130 μm along the axial direction, respectively (Figure 2a,c). The content of LTO and LMO was confirmed to be 78% and 90% in weight by thermogravimetric analysis. The LTO and LMO nanoparticles were evenly dispersed and incorporated within the aligned MWCNTs, which effectively served as skeletons (Figure 2b,d; see also Figure S3 and S4). The composite yarns were lightweight, with linear densities of 2 and 10 mg m^{-1} for the MWCNT/LTO and MWCNT/LMO yarns, respectively, and highly flexible (Figure S5).

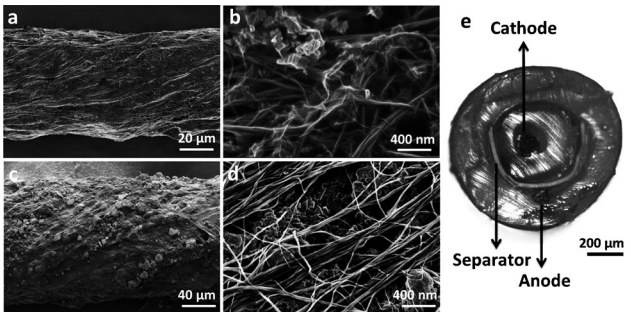

Figure 2. Characterization of the wire-shaped battery. a,b) SEM images of an MWCNT/LTO composite yarn at low (a) and high (b) magnification. c,d) SEM images of an MWCNT/LMO composite yarn at low (c) and high (d) magnification. e) Cross-sectional micrograph of a full cell.

The alignment is advantageous to extend the excellent mechanical and electronic properties of individual MWCNTs to the macroscopic scale. The composite yarns were flexible and strong, and they can be deformed into various shapes without obvious structural damage. In particular, the aligned and continuous MWCNTs functioned as effective pathways for charge transport and served as current collectors, which endowed the composite yarns with remarkable electrochemical properties. They were investigated in half-cells with lithium wires as the counter electrodes. Typical charge and discharge curves of the aligned MWCNT/LTO and MWCNT/LMO composite yarns with a length of 1 cm at a current of 0.02 mA are shown in Figure 3a and 3c, respectively. Accordingly, the specific capacities per gram of the two composite yarns were calculated as 150 and 60 mAh g^{-1}, which are lower than the theoretical values of 175 and 135 mAh g^{-1} for bare LTO and LMO, respectively. The discharge plateau was generated at 1.5 V for the MWCNT/LTO yarn, and a charge plateau was observed at approximately 4.0 V for the MWCNT/LMO yarn.

Galvanostatic charge–discharge measurements were conducted to study the stability of the two composite yarns at a current of 0.05 mA (Figure 3b,d). Both yarns were able to retain more than 80% of their capacities after 200 cycles. The surface of the MWCNT/LTO composite yarn was coated with a thin layer of graphene oxide to enhance the structure stability (Figure 2a,c). In contrast, a low capacity retention of 60% was observed without the graphene oxide coating under the same conditions (Figure S6). The MWCNT/LTO composite yarn also exhibited a good rate performance: 0.0043, 0.0037, and 0.0023 mAh cm^{-1} at currents of 0.02, 0.05, and 0.1 mA, respectively (Figure S7). This excellent performance is due to the remarkable electrochemical properties of the LTO nanoparticles and intimate contacts between the LTO nanoparticles and the MWCNTs (Figure 2b). For the MWCNT/LMO composite yarn, the LMO nanoparticles were comparatively smaller. It was found that a more effective method for the preparation of this composite yarn entailed the addition of a proportion of the MWCNT powder to the LMO suspension. The added MWCNTs formed a network structure (Figure 2d; see also Figure S8). The discharge capacity dropped from 0.0038 to 0.000035 mAh cm^{-1} with an increase in current from 0.02 to 0.1 mA without the networked MWCNTs (Figure S9) as the LMO nanoparticles cannot be stably anchored by the aligned MWCNTs alone. In contrast, the MWCNT/LMO composite yarn showed a much better performance with charge capacities of 0.0082, 0.00031, and 0.00018 mAh cm^{-1} at 0.02, 0.05, and 0.1 mA, respectively.

The plateau difference and stable electrochemical performances of the two composite yarns make them promising electrode materials for metallic-lithium-free batteries. The electrode reaction can be expressed as Equations (1) and (2).

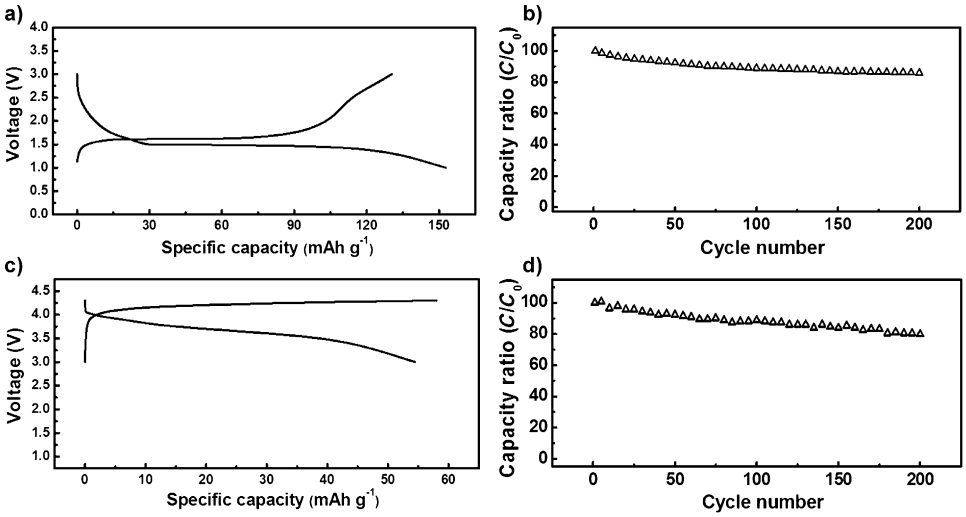

Figure 3. Electrochemical properties of aligned MWCNT/LTO and MWCNT/LMO composite yarns compared to those of a lithium wire. a) Charge–discharge curves at 0.02 mA and b) capacity retention at 0.05 mA of the aligned MWCNT/LTO half-cell with a length of 1 cm. c) Charge–discharge curves at 0.02 mA and d) capacity retention at 0.05 mA of the aligned MWCNT/LMO half-cell with a length of 1 cm.

During the charge process, lithium ions are removed from the $LiMn_2O_4$ lattice, transferred into the electrolyte, and intercalated into the $Li_4Ti_5O_{12}$ lattice at the anode. This process is reversed during discharge. Therefore, the lithium ions shuttle between the two electrodes, while the electrons flow through the external circuit during the charge/discharge process.

Reaction at the cathode :

$$LiMn_2O_4 \leftrightarrow Li_{1-x}Mn_2O_4 + x\,Li^+ + x\,e^- \quad (1)$$

Reaction at the anode :

$$Li[Li_{1/3}Ti_{5/3}]O_4 + x\,Li^+ \leftrightarrow Li_{1+x}[Li_{1/3}Ti_{5/3}]O_4 \quad (2)$$

The aligned MWCNT/LTO and MWCNT/LMO composite yarns were assembled with a belt separator between them to form the wire-shaped lithium-ion battery. The battery was sealed in a heat-shrinkable tube with a diameter of 1.2 mm, as shown in the cross-sectional micrograph (Figure 2e). With the resulting wire-shaped full battery, a galvanostatic discharge–charge measurement was conducted. Figure 4a shows typical voltage profiles of charge and discharge at a current of 0.05 mA, exhibiting a reversible capacity of 70 mAh g^{-1} (limited by the MWCNT/LTO composite). The discharge plateau voltage slightly decreased from 2.5 to 2.2 V with increasing current densities (Figure 4b), which evidently revealed that the wire-shaped battery can stably operate at high current densities.

The full cell achieved a high specific capacity of 0.0028 mAh cm^{-1} (138 mAh g^{-1}) at 0.01 mA (limited by the MWCNT/LTO composite). The wire-shaped batteries delivered a discharge volumetric energy density of 17.7 mWh cm^{-3} based on the overall volume of anode and cathode, which is higher than those of planar lithium thin-film batteries (1–10 mWh cm^{-3})[26,29] and two or more orders of magnitude larger than that of wire-shaped supercapacitors.[9,30,31] They demonstrated a high power density of 0.56 W cm^{-3}, which is an order of magnitude larger than the power density of lithium thin-film batteries (10^{-2}–10^{-3} W cm^{-3}).[26,29] The full cell also showed a stable galvanostatic charge–discharge performance, certified by a capacity retention of 85% after 100 cycles at 0.05 mA and a coulombic efficiency of 80% (Figure 4c; see also Figure S10). The morphology of the fiber electrode was well maintained after continuous charge–discharge processes, and a thin layer of solid electrolyte interphase was produced on the electrode surface (Figure S11). The capacity retention deteriorated at or beyond 0.1 mA (Figure S12). The wire-shaped battery was flexible and can be deformed into various shapes without physical damage and with negligible performance loss (Figure 5a). As shown in Figure 5b, the voltage profiles were perfectly maintained even after repeating the bending testes 1000 times.

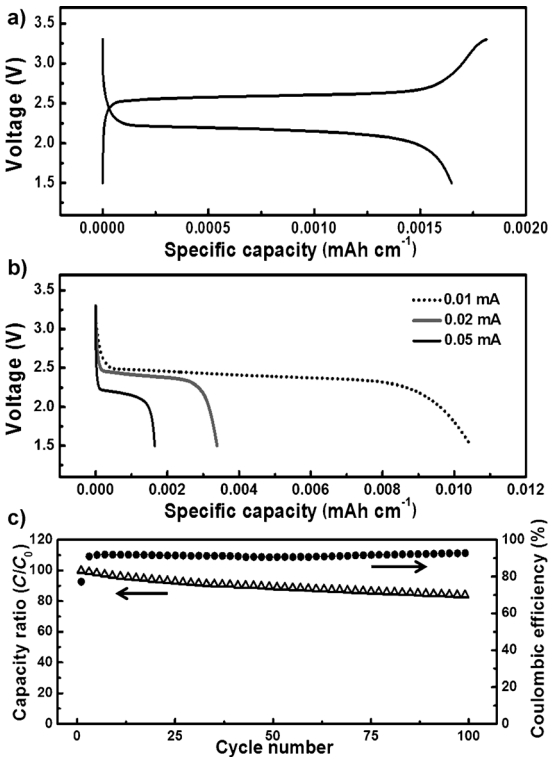

Figure 4. Electrochemical performance of the wire-shaped full cell with a length of 1 cm. a) Galvanostatic charge and discharge curves at 0.05 mA. b) Discharge profiles at different currents. c) Capacity retention and coulombic efficiency after 100 charge–discharge cycles at 0.05 mA.

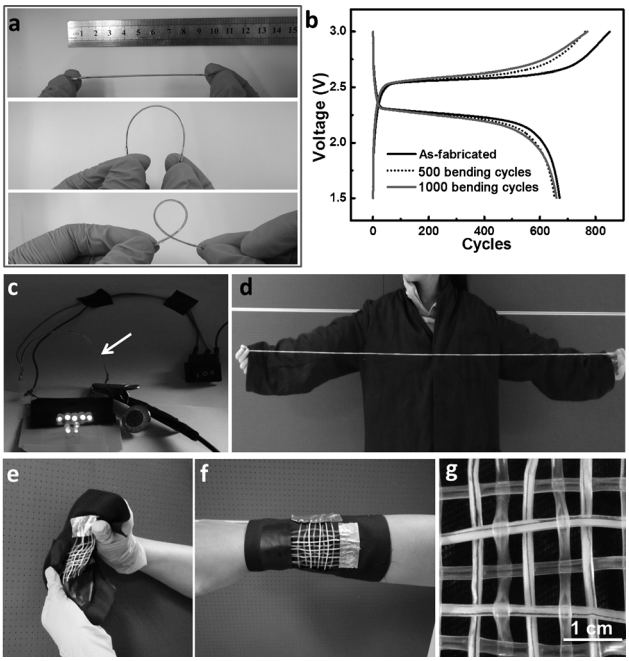

Figure 5. Flexibility of wire-shaped lithium-ion batteries. a) Photographs of a wire-shaped battery being deformed into different shapes. b) Galvanostatic charge and discharge curves before and after bending for 500 and 1000 cycles at 0.05 mA. c) Nine light-emitting diodes being powered by a wire-shaped battery with a length of 10 cm. d) A long wire-shaped lithium ion battery with a length of 200 cm. e–g) Wire-shaped batteries woven into flexible textiles.

A fully charged wire-shaped battery with a length of 10 cm and a weight of 0.08 g was capable of lighting up nine red light-emitting diodes (LEDs) for at least 60 seconds (Figure 5c). Furthermore, the illumination intensity of the nine LEDs remained steady even when the wire-shaped battery was bent into various shapes (Movie S1). Furthermore, a red LED could be steadily lighted for one minute with a 2.5 cm wire-shaped battery bent into a ring (Figure S13). This wire-shaped battery can also be manufactured on a large scale, and a long wire-shaped battery with a length of 200 cm is shown in Figure 5d. The wire-shaped battery was woven into various flexible structures, such as electronic textiles, which are expected to satisfy the ever-growing requirements for portable electronics (Figure 5e–g-)

An elastic wire-shaped lithium-ion battery was further fabricated by winding the yarn cathode and anode around an elastic substrate (Figure 6a; see also Figure S14), followed by coating with a thin layer of gel electrolyte to obtain a highly stretchable spring structure. The stretchable battery was also highly flexible and can be readily distorted without physical damage (Figure S15). The elastic wire-shaped battery was used to power a red LED (Figure 6b; see also Video S2). No obvious change in the illumination intensity of the LED was observed when the battery was continuously stretched by 100%. The electrochemical performance of the stretchable lithium ion battery was investigated under increasing elongations from 0, 20, 40, 60, 80, to 100%. As a result, the specific capacity exhibited a moderate loss, but still remained at over 90% when the battery was stretched by 100% (Figure 6c), and the shapes of the charge–discharge curves were also perfectly retained (Figure S16). After 200 cycles of stretching by 100%, the specific capacity remained at over 80% (Figure 6d). The wire-shaped battery can be stretched by 100% because of its spring-like configuration (Figure S17) as well as the elastic substrate and gel electrolyte. The structure integrity of the yarn electrodes under stretching was verified by tracing the change in the electrical resistance during stretching (Figure S18). The resistances for both composite yarns fluctuated within 1% when stretched by 100%. The maximum strain of the battery depends on the stretchability of the substrate; a strain of up to 600% could be achieved with an elastic polydimethylsiloxane

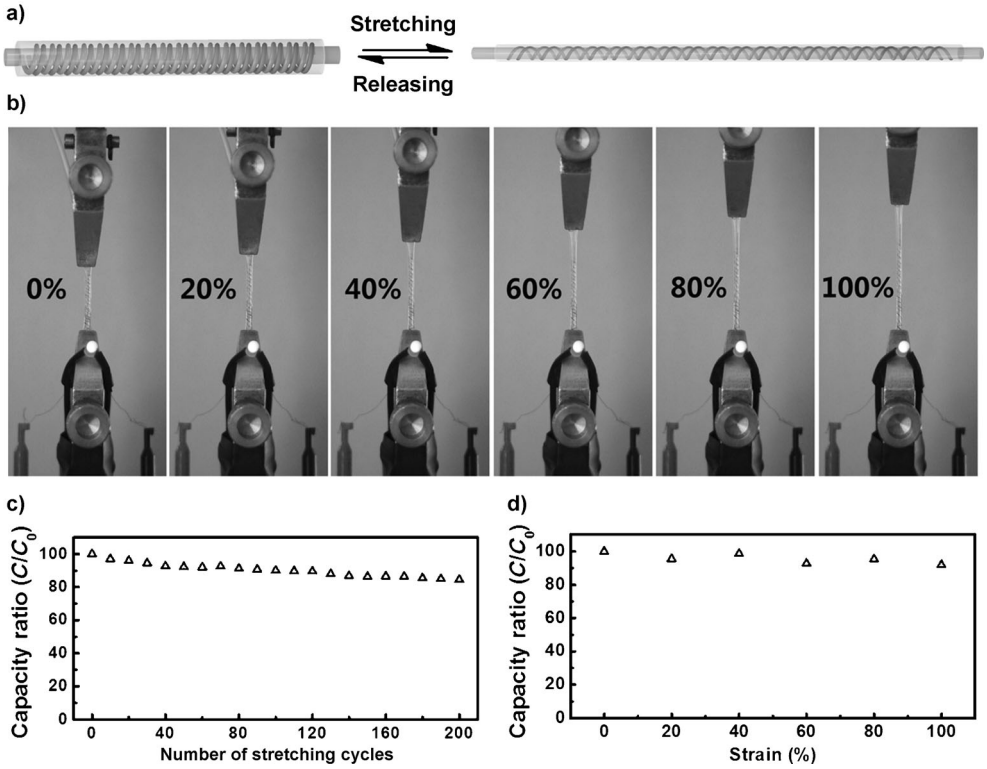

Figure 6. Elastic wire-shaped lithium-ion batteries. a) Stretching and releasing process. b) Photographs of a battery used to power a light-emitting diode at increasing strains. c) Dependence of the specific capacity on strain. d) Dependence of the specific capacity on the number of stretching cycles with a strain of 100%. C_0 and C correspond to the specific capacities before and after stretch.

substrate. Details of this investigation will be reported in due course.

In summary, novel wire-shaped full lithium-ion batteries were fabricated by assembling two composite yarn electrodes that exhibited remarkably mechanical, electrical, and electrochemical properties. The wire-shaped batteries are safe because of the two well paired electrodes that are free of metallic lithium. They also showed high volumetric energy densities and power densities at high charge and discharge rates. The wire-shaped batteries were light and flexible and can be produced on a large scale by a continuous fabrication method with high efficiency. Moreover, they were woven into deformable and stable electronic textiles. Furthermore, by simply winding the yarn cathode and anode around an elastic substrate, a spring structure was created to obtain a stretchable battery that displays considerable capacity retention even when stretched by up to 100%. The combined properties make these materials suitable for a wide range of applications in wearable and portable electronics.

Experimental Section

Synthesis of composite yarns: LMO nanoparticles were synthesized by a hydrothermal method. LiOH (0.377 g) and MnO_2 (1.37 g) were first dissolved in H_2O (40 mL); then glucose (0.2 g) and H_2O (40 mL) were added, and the resulting mixture reacted at 200 °C for 24 h. The obtained LMO nanoparticles (75 mg) and MWCNT powder (10–20 μm, 7.5 mg) were then dispersed in *N*,*N*-dimethylformamide (15 mL) to obtain a suspension. Aligned MWCNT arrays were synthesized by typical chemical vapor deposition. MWCNT sheets with a thickness of ca. 18 nm were drawn out of the arrays with a width of ca. 2 cm. Two MWCNT sheets stacked along the drawing direction were immersed into the MWCNT/LMO suspension, the solvent was subsequently volatilized, and the material rolled into yarns. LTO nanoparticles were synthesized by a solid-state method. TiO_2 (anatase, 8 nm) and Li_2CO_3 were mixed in a molar ratio of 2.5 and then heated at 800 °C for 24 h under N_2 atmosphere to obtain well-crystallized $Li_4Ti_5O_{12}$ (LTO). The resulting LTO powder was further treated by a ball-milling machine (Fritsch Pulverisette 6) for 20 h to form LTO nanoparticles. LTO nanoparticles (75 mg) were dispersed in *N*,*N*-dimethylformamide (15 mL). Two MWCNT sheets stacked along the drawing direction (2 cm in width) were immersed into the LTO suspension and then rolled into composite yarns. The MWCNT/LTO composite yarn was further passed through an aqueous solution of graphene oxide (0.5 wt%) to coat a thin graphene oxide layer onto the yarn surface. The graphene oxide sheets were synthesized according to a modification of Hummer's method.[32]

Fabrication of wire-shaped batteries: A half-cell was made by assembling a composite yarn and a lithium wire with a separator between them to prevent the short circuit. $LiPF_6$ (1M) in a solvent mixture of ethylene carbonate, diethyl carbonate, and dimethyl carbonate (1:1:1, w/w) was used as the electrolyte. To make a full cell, the composite-yarn anode and cathode were inserted into a heat-shrinkable tub with a separator between them and heated with a heat gun at 120 °C for 1 min to shrink the tube. Finally, the electrolyte was injected into the tube in an argon-filled glove box.

Electrochemical analysis: The electrochemical performances were measured with an Arbin electrochemical station (MSTAT-5 V/10 mA/16Ch). The full cell was charged from 1.5 to 3.3 V at currents of 0.01, 0.02, 0.05, and 0.1 mA. The LTO-based half-cell was charged from 1 to 3 V, and the LMO-based half-cell was charged from 3 to 4.3 V, both at currents of 0.01, 0.02, 0.05, and 0.1 mA. The length- and mass-specific capacities (C_L and C_m) were calculated from the charge and discharge profiles according to $C_L = (I\Delta t)/L$ and $C_m = (I\Delta t)/m$, where I, Δt, L, and m correspond to the applied current (A), discharge time (s), effective yarn length (cm), and the mass of the anode electrode (g), respectively. The mass-specific capacity of the full battery was specified by the MWCNT/LTO electrode. The calculations of the power and energy densities were based on the overall mass and volume of cathode and anode.

Fabrication of the stretchable battery: The gel electrolyte was first prepared in a glove box filled with dry Argon. Poly(ethylene oxide) (average molecular weight ca. 600000, 0.35 g) was added to a CH_2Cl_2/acetone mixture (40:1, w/w); then succinonitrile (0.35 g) and lithium bis(trifluoromethane)sulfonimide (LiTFSI; 0.30 g) were added. A clear gel electrolyte was obtained after stirring for 5 h. The yarn cathode and anode were assembled in parallel at a distance of ca. 0.2 cm on a motorized translation stage. Two ends of an elastic heat-shrinkable tube (Shanghai Wei Cheng Electronics Lt.Co.) were fixed on two motors at an angle of 60° to the translatory direction. The heat-shrinkable tube exhibited a Young's modulus of 5.6 MPa (Figure S19). The translation stage and two motors were simultaneously moved so that the two composite yarns were twisted onto the heat-shrinkable tube. The velocity of the translation stage was 1.7 times faster than the linear velocity of the two motors to maintain the helical angle of 60°. The resulting yarn was finally coated with a thin layer of gel electrolyte in the glove box and inserted into another heat-shrinkable tube, followed by heating to seal the two ends (120 °C for 1 min) to produce the wire-shaped battery.

Received: February 13, 2014
Revised: May 5, 2014
Published online: June 4, 2014

Keywords: carbon-based materials · electrochemistry · lithium-ion batteries · nanotubes

[1] M. C. McAlpine, H. Ahmad, D. W. Wang, J. R. Heath, *Nat. Mater.* **2007**, *6*, 379–384.
[2] S. Y. Lee, K. H. Choi, W. S. Choi, Y. H. Kwon, H. R. Jung, H. C. Shin, J. Y. Kim, *Energy Environ. Sci.* **2013**, *6*, 2414–2423.
[3] G. S. Jeong, D. H. Baek, H. C. Jung, J. H. Song, J. H. Moon, S. W. Hong, I. Y. Kim, S. H. Lee, *Nat. Commun.* **2012**, *3*, 977.
[4] Y. F. Li, *Acc. Chem. Res.* **2012**, *45*, 723–733.
[5] I. Kovalenko, B. Zdyrko, A. Magasinski, B. Hertzberg, Z. Milicev, R. Burtovyy, I. Luzinov, G. Yushin, *Science* **2011**, *334*, 75–79.
[6] Y. H. Kwon, S. W. Woo, H. R. Jung, H. K. Yu, K. Kim, B. H. Oh, S. Ahn, S. Y. Lee, S. W. Song, J. Cho, H. C. Shin, J. Y. Kim, *Adv. Mater.* **2012**, *24*, 5192–5197.
[7] D. J. Lipomi, B. C. K. Tee, M. Vosgueritchian, Z. N. Bao, *Adv. Mater.* **2011**, *23*, 1771–1775.
[8] T. Yamada, Y. Hayamizu, Y. Yamamoto, Y. Yomogida, A. Izadi-Najafabadi, D. N. Futaba, K. Hata, *Nat. Nanotechnol.* **2011**, *6*, 296–301.
[9] J. Ren, L. Li, C. Chen, X. L. Chen, Z. B. Cai, L. B. Qiu, Y. G. Wang, X. R. Zhu, H. S. Peng, *Adv. Mater.* **2013**, *25*, 1155–1159.
[10] J. A. Lee, M. K. Shin, S. H. Kim, H. U. Cho, G. M. Spinks, G. G. Wallace, M. D. Lima, X. Lepro, M. E. Kozlov, R. H. Baughman, S. J. Kim, *Nat. Commun.* **2013**, *4*, 1970.
[11] Y. P. Fu, X. Cai, H. W. Wu, Z. B. Lv, S. C. Hou, M. Peng, X. Yu, D. C. Zou, *Adv. Mater.* **2012**, *24*, 5713–5718.
[12] X. H. Lu, T. Zhai, X. H. Zhang, Y. Q. Shen, L. Y. Yuan, B. Hu, L. Gong, J. Chen, Y. H. Gao, J. Zhou, Y. X. Tong, Z. L. Wang, *Adv. Mater.* **2012**, *24*, 938–944.
[13] Z. B. Yang, J. Deng, X. L. Chen, J. Ren, H. S. Peng, *Angew. Chem.* **2013**, *125*, 13695–13699; *Angew. Chem. Int. Ed.* **2013**, *52*, 13453–13457.

[14] X. L. Chen, L. B. Qiu, J. Ren, G. Z. Guan, H. J. Lin, Z. T. Zhang, P. N. Chen, Y. G. Wang, H. S. Peng, *Adv. Mater.* **2013**, *25*, 6436 – 6441.
[15] S. Megahed, B. Scrosati, *J. Power Sources* **1994**, *51*, 79 – 104.
[16] Y. K. Sun, D. H. Kim, C. S. Yoon, S. T. Myung, J. Prakash, K. Amine, *Adv. Funct. Mater.* **2010**, *20*, 485 – 491.
[17] J. Hassoun, S. Panero, P. Reale, B. Scrosati, *Adv. Mater.* **2009**, *21*, 4807 – 4810.
[18] Z. H. Chen, Y. Ren, A. N. Jansen, C. K. Lin, W. Weng, K. Amine, *Nat. Commun.* **2013**, *4*, 1513.
[19] M. Armand, J. M. Tarascon, *Nature* **2008**, *451*, 652 – 657.
[20] G. Armstrong, A. R. Armstrong, P. G. Bruce, P. Reale, B. Scrosati, *Adv. Mater.* **2006**, *18*, 2597 – 2600.
[21] J. Gao, J. R. Ying, C. Y. Jiang, C. R. Wan, *J. Power Sources* **2007**, *166*, 255 – 259.
[22] P. Gibot, M. Casas-Cabanas, L. Laffont, S. Levasseur, P. Carlach, S. Hamelet, J. M. Tarascon, C. Masquelier, *Nat. Mater.* **2008**, *7*, 741 – 747.
[23] Y. G. Wang, H. M. Liu, K. X. Wang, H. Eiji, Y. R. Wang, H. S. Zhou, *J. Mater. Chem.* **2009**, *19*, 6789 – 6795.
[24] G. N. Zhu, Y. G. Wang, Y. Y. Xia, *Energy Environ. Sci.* **2012**, *5*, 6652 – 6667.
[25] L. N. Wang, K. Nakura, M. Imazaki, N. Kakizaki, K. Ariyoshi, T. Ohzuku, *J. Electrochem. Soc.* **2012**, *159*, A1710 – A1715.
[26] D. Pech, M. Brunet, H. Durou, P. H. Huang, V. Mochalin, Y. Gogotsi, P. L. Taberna, P. Simon, *Nat. Nanotechnol.* **2010**, *5*, 651 – 654.
[27] L. Cheng, X. L. Li, H. J. Liu, H. M. Xiong, P. W. Zhang, Y. Y. Xia, *J. Electrochem. Soc.* **2007**, *154*, A692 – A697.
[28] Y. Y. Liang, S. J. Bao, B. L. He, W. J. Zhou, H. L. Li, *J. Electrochem. Soc.* **2005**, *152*, A2030 – A2034.
[29] Z. S. Wu, K. Parvez, X. L. Feng, K. Mullen, *Nat. Commun.* **2013**, *4*, 2487.
[30] J. Bae, M. K. Song, Y. J. Park, J. M. Kim, M. L. Liu, Z. L. Wang, *Angew. Chem.* **2011**, *123*, 1721 – 1725; *Angew. Chem. Int. Ed.* **2011**, *50*, 1683 – 1687.
[31] J. Ren, W. Y. Bai, G. Z. Guan, Y. Zhang, H. S. Peng, *Adv. Mater.* **2013**, *25*, 5965 – 5970.
[32] Z. Yang, H. Sun, T. Chen, L. Qiu, Y. Luo, H. Peng, *Angew. Chem.* **2013**, *125*, 7693 – 7696; *Angew. Chem. Int. Ed.* **2013**, *52*, 7545 – 7548.

